



HAL
open science

Living in the Canopy of the Animal Forest: Physical and Biogeochemical Aspects

Katell Guizien, Marco Ghisalberti

► **To cite this version:**

Katell Guizien, Marco Ghisalberti. Living in the Canopy of the Animal Forest: Physical and Biogeochemical Aspects. Sergio Rossi; Lorenzo Bramanti; Andrea Gori; Covadonga Orejas. Marine Animal Forests. The Ecology of Benthic Biodiversity Hotspots, Springer International Publishing, pp.1-22, 2016, 10.1007/978-3-319-17001-5_14-1 . hal-03999703

HAL Id: hal-03999703

<https://hal.science/hal-03999703v1>

Submitted on 21 Feb 2023

HAL is a multi-disciplinary open access archive for the deposit and dissemination of scientific research documents, whether they are published or not. The documents may come from teaching and research institutions in France or abroad, or from public or private research centers.

L'archive ouverte pluridisciplinaire **HAL**, est destinée au dépôt et à la diffusion de documents scientifiques de niveau recherche, publiés ou non, émanant des établissements d'enseignement et de recherche français ou étrangers, des laboratoires publics ou privés.

1 Living in the Canopy of the Animal forest: Physical and Biogeochemical Aspects

2

3 Katell GUIZIEN

4

5 Sorbonne Universités, CNRS, UPMC Univ Paris 06, Laboratoire d'Ecogéochimie des
6 Environnements Benthiques (LECOB), Observatoire Océanologique, F-66650, Banyuls/Mer,
7 France

8 e-mail : guizien@obs-banyuls.fr

9

10 Marco GHISALBERTI

11

12 Department of Infrastructure Engineering, University of Melbourne, Parkville, Melbourne, Victoria
13 3010, Australia

14

15 School of Civil, Environmental and Mining Engineering, University of Western Australia, Perth,
16 WA 6009, Australia

17

18

19 Contents

20

21 1. Introduction

22

23 2. The hydrodynamics above and inside the marine animal forest

24

25 3. The biogeochemistry above and inside the marine animal forest

26

27 4. Living in the canopy of animal forest

28

29 5. Conclusions and future directions

30

31

32

33

34

35

36 Abstract

37

38 Long-lived hard and soft coral species that are able to develop dense patches with a complex, three-
39 dimensional structure form an animal forest canopy, similar to trees in terrestrial systems. Aside
40 from the shelter provided by this canopy to other organisms, the animal forest can significantly
41 modify the local physical and biogeochemical environment.

42 In the first part of this chapter, the modification of benthic boundary layer hydrodynamics in and
43 above canopies is described, with a focus on the impacts of canopy density and flexibility. In the
44 second part of this chapter, the structure of diffusive and advective mass transfer in canopies will be
45 presented and discussed in relation to the biogeochemical transformations observed in animal forest
46 canopies. Ongoing challenges in the conceptualisation of physical and biogeochemical processes in
47 animal forest canopies are also exposed. In the third part of this chapter, we review the factors that
48 form the basis of a mechanistic explanation of the development of micro-niches, which explain the
49 large diversity hosted in animal forest canopies.

50

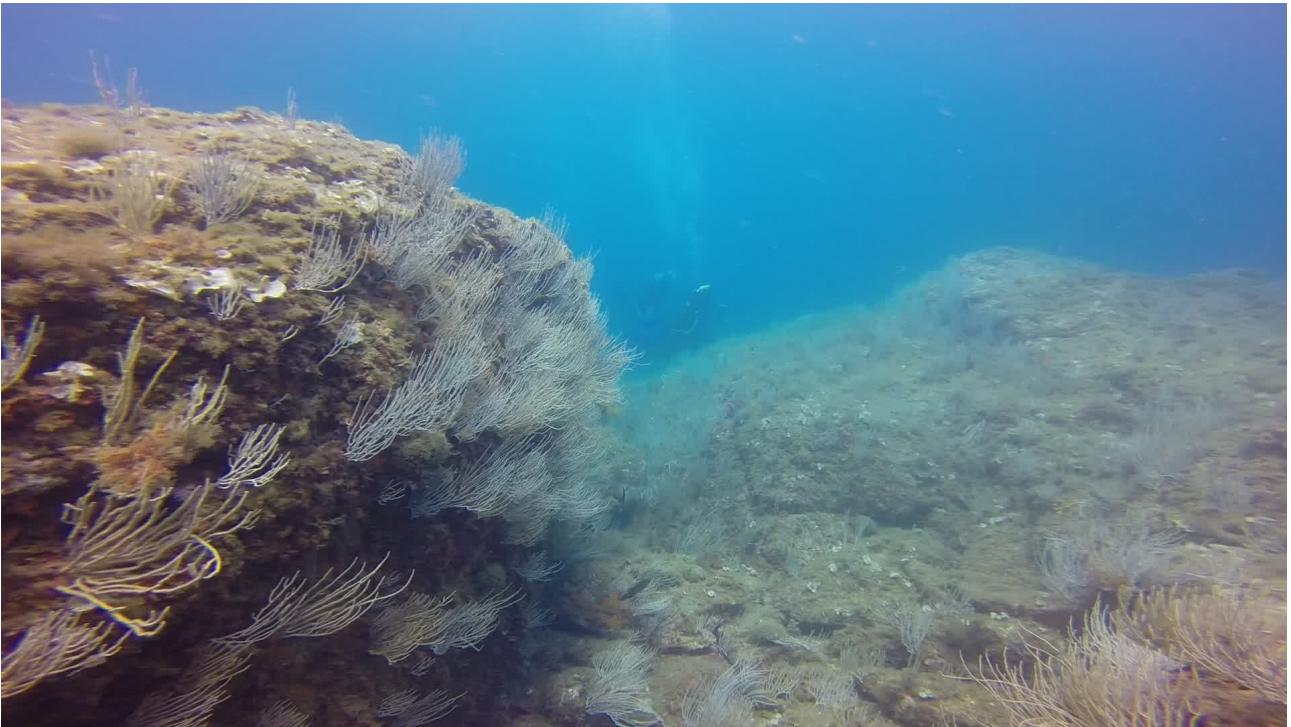
51 Keywords : Benthic boundary layer, flow instability, drag, micro-niche, spatial heterogeneity,
52 gradients, filaments, biotic-abiotic interactions, ecosystem engineers

53

54 1. Introduction

55

56 The concept of the ‘marine animal forest’ was initially introduced based on aesthetic similarities
57 between trees and large erect colonial animal communities (e.g. corals, Bruno and Bertness, 2001)
58 that cover some marine substrates (see Figure 1, as well as Gutt et al. in this book). Similarly to
59 terrestrial forests, marine animal forests form a sheltered habitat by reducing the foraging efficiency
60 of consumers (Bartholomew 2000; Beukers and Jones 1997) and providing refuge for motile
61 species like fishes or vagile invertebrates (Ross and Quattrini 2007). The similarities between
62 marine and terrestrial forests extend beyond the provision of shelter, however, and include the
63 manner in which these systems modify the local physical and biogeochemical environment. Despite
64 differences in spatial scale and the properties (density, viscosity, heat capacity) of the fluid to which
65 they are exposed, steady flows over atmospheric ($O(10-100\text{ m})$) and aquatic canopies ($O(0.1-1\text{ m})$)
66 display a common characteristic flow structure, as detailed in Section 2. Because of such
67 similarities, we use the terms ‘forest’ and ‘canopy’ interchangeably here.



70 Figure 1: The white gorgonian, *Eunicella singularis*, covering a boulder at 15 meters depth in Cap
71 L'Abeille (Réserve Naturelle Marine de Cerbère-Banyuls, NW Mediterranean sea, Photograph by
72 Katell Guizien).

73

74 Organisms forming canopies are typically considered ‘ecosystem engineers’, a term which refers to
75 organisms that, through causing changes in the local physical or biogeochemical conditions, directly
76 or indirectly control the availability of resources (other than themselves) to other organisms and
77 thus, modify, maintain or create habitats (Lawton, 1994). Autogenic engineers modify their
78 environment through physical changes, while allogenic engineers do so through chemical
79 transformations (Jones et al. 1997). Six factors have been identified by Jones et al. (1997) as
80 defining the scale of impact of an ecosystem engineer: (1) the lifetime activity of individual
81 organisms, (2) the population density and size, (3) the spatial distribution of the population, both at
82 the local and regional level, (4) the length of time a population has been present at a site, (5) the
83 durability of constructs, artifacts and impacts in the absence of the original engineer, and (6) the
84 number and types of resource flows that are modulated by the constructs and artifacts, and the
85 number of other species dependent upon these flows. On the basis of these factors, trees have

86 always been considered the paradigmatic example of ecosystem engineers in terrestrial habitats
87 (Holling 1992).

88 Marine animal forests have been shown to act as autogenic ecosystem engineers in marine systems
89 through the provision of habitat, colonization opportunities and increasing habitat complexity. For
90 corals, these effects are well-established in shallow tropical environments, but also recognized in
91 temperate (Scinto et al. 2009 ; Cerrano et al. 2010) and deep-water environments (Cordes et al.
92 2008; Freiwald and Roberts 2005). Animal forests also act as autogenic ecosystem engineers
93 through modification of the mean and turbulent flow structure. The lower levels of turbulence
94 inside the canopy increase sedimentation (Luckenbach 1986), causing the retention of propagules
95 and enhancing larval settlement (Eckman 1985; Smith and Witman 1999; Bruno 2000). At the top
96 of the canopy, the enhanced turbulence generated by the large canopy roughness augments the
97 delivery of food and critical metabolites by reducing the thickness of the diffusive boundary layer
98 on organism surfaces (Dennison and Barnes 1988; Thisle and Eckman 1990; Shashar et al. 1996).
99 Flow modification by marine forests encompasses a wide range of processes on a range of spatial
100 scales (reviewed for coral reefs by Monismith 2007) and it is now clear that the hydrodynamics of
101 marine forests demonstrate strong similarities, regardless of whether the forest is comprised of
102 plants (e.g. kelp forests or seagrass meadows, Eckman et al. 1989; Duarte 2000) or animals. This
103 flow modification likely leads to the creation of highly dynamic micro-environments, which
104 ultimately select those organisms able to feed, grow and reproduce within the marine forest.

105 Animal marine forests can also act as allogenic ecosystem engineers, although in the opposite
106 manner to vegetation canopies. Indeed, marine forests of autotrophic primary producers are
107 expected to be carbon sinks (like their terrestrial counterparts) through atmospheric carbon fixation
108 by photosynthesis (Goreau 1992). In contrast, marine forests of heterotrophic consumers (except
109 corals living in symbiosis with autotrophic algae) release inorganic carbon during organic matter
110 assimilation in respiration. Nevertheless, the allogenic impact of the 'wall of mouths' of marine
111 animal forests is expected to significantly alter the local biogeochemical conditions near the sea
112 floor (Fabricius and Metzner 2004).

113 The objective of this chapter is to review the state-of-the-art understanding of the hydrodynamics
114 and biogeochemistry of marine animal forests and their impact on living conditions inside the ani-
115 mal forest.

116

117 2. The hydrodynamics inside and above the marine animal forest

118

119 Marine animal forests can be found in both shallow and deep environments, exposing them to a
120 range of hydrodynamic conditions in terms of the magnitude and steadiness of the flow. At the
121 marine forest scale, steady flows include those generated by wind, buoyancy or tides, with surface
122 waves (seas and swell) generating an unsteady flow. Flow in the oceanic bottom boundary layer is
123 therefore often decomposed into a quasi-steady unidirectional component (the current) and a series
124 of periodic components (waves). This decomposition is of utmost importance when considering the
125 hydrodynamics inside and above the marine animal forest, as the bottom boundary layers associated
126 with steady and unsteady flows differ greatly in their size and structure.

127

128 *Structure of the turbulent boundary layer over flat beds in steady flows*

129

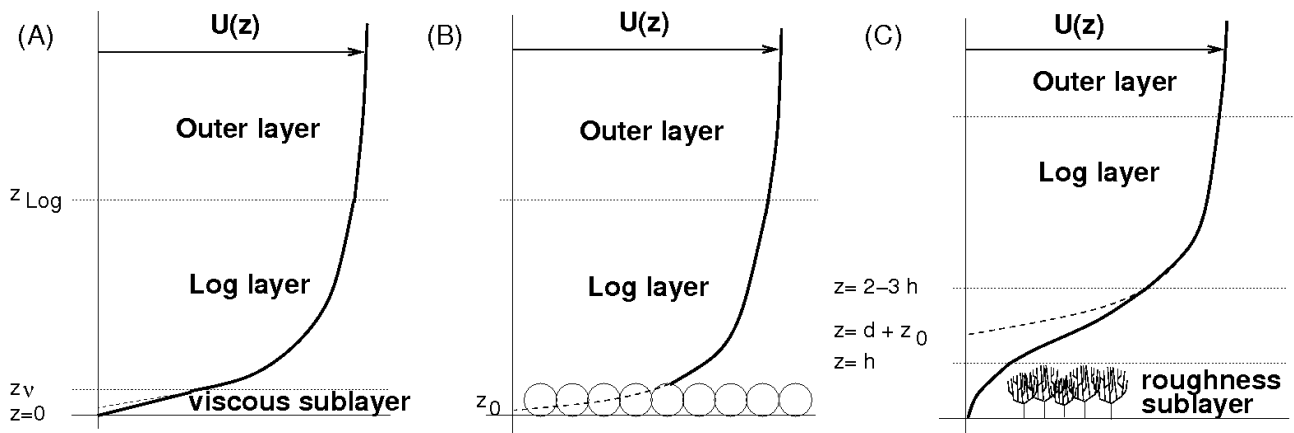
130 The bottom boundary layer is the region where the flow velocity is impacted by the bed and where
131 flows dissipate their energy into heat by viscous friction to reach a zero velocity at the bottom.
132 Under unidirectional steady flows, the thickness (δ) of a turbulent boundary layer decreases with
133 flow energy and is roughly given by $\delta \approx 6000\nu/u_*$ (Wilcox 1992) where ν is the kinematic viscosity
134 and u_* the bottom friction velocity (defined as the square root of the bed shear stress divided by fluid
135 density). This yields a typical value of $\delta \sim O(m)$ for $u_* \sim O(cm/s)$. The flow in a steady turbulent
136 boundary layer exhibits a well-known vertical structure, with three distinct regions (Wilcox 1992):
137 (1) the viscous sublayer nearest the bed, where the velocity is low and viscous forces dominate
138 inertial forces, (2) the logarithmic (or inertial) layer, where viscous forces are progressively
139 overwhelmed by inertial forces, and (3) the outer layer, where the flow velocities are greatest, and
140 exceed the bottom friction velocity by at least an order of magnitude. (Figure 2A). The viscous
141 sublayer and logarithmic layer form the inner part of the boundary layer, where the flow velocity
142 scales on the bottom friction velocity. In the viscous sublayer, velocity increases linearly with
143 distance from the bed up to $z_v \approx 30 \nu/u_*$. In the logarithmic layer (of $O(10 \text{ cm})$ in height for the
144 typical flow considered above), the velocity increases logarithmically with distance from the bed
145 according to the 'law of the wall' (Figure 2A). Over a rough bed, the viscous sublayer can vanish
146 between roughness elements (Figure 2B). This is seen when $u_*k/\nu > 70$ (Sleath 1984), where k is the
147 average height of the roughness elements ($k \approx 30 z_0$, Nikuradse 1933), and the law of the wall can
148 be expressed as :

$$149 \quad U(z) = u_*/\kappa \ln [z/z_0] \quad \text{for } k_N < z < z_{Log}=600 \nu/u_* \quad (1)$$

150 where $\kappa = 0.41$ is the von Karman constant.

151 In the outerlayer, velocity do not have as a simple formulation as in the viscous and Log layers.

152



154 Figure 2: Schematic diagram of the vertical structure of the mean velocity in (A) a smooth-bottom
155 boundary layer, (B) a rough-bottom boundary layer, and (C) a canopy boundary layer formed by
156 obstacles of height h .

157

158 *Structure of the turbulent boundary layer over large obstacles in steady flows: the canopy effect*

159

160 When ocean beds are covered by large obstacles (i.e. a canopy) which extend into the theoretical
161 logarithmic layer of the unobstructed flow, the classical boundary layer structure can be
162 significantly modified when obstacles height is larger than 10 % of its drag length scale (see
163 definition below, Nepf et al. 2007). This is typically the case in animal forests formed by erect
164 organisms larger than a few centimeters. The wakes produced by these obstacles create strong
165 spatial variations in the flow, over a region (embedded within the boundary layer) known as the
166 roughness sublayer (RSL, Figure 2C). In an homogeneous canopy (of elements of height h), the
167 RSL is estimated to extend to approximately $2-3h$ above the bed (MacDonald 2000). Above the
168 RSL, where the flow is horizontally homogeneous, there is again a logarithmic dependence of
169 velocity on height; the profile in (1) is shifted upwards by a displacement height, d (Raupach et al.,
170 1980). Within the canopy (i.e. in the lower part of the roughness sublayer, below $z = h$), the vertical
171 profile of horizontally-averaged flow velocity has been approximated by an exponential decay from
172 its value at the top of the canopy (U_h) down to the bed (MacDonald 2000, Cheng and Castro 2002).
173 The mean flow velocity, $U(z)$, inside and above animal forests is thus typically modelled as:

174

175 $U(z) = u_*/\kappa \ln [(z-d) / z_0]$ for $z > 2-3h$ (2)

176 $= U_h \exp [\alpha(z/h - 1)]$ for $0 < z < h$ (3)

177

178 where z is the distance from the bottom, u_* is the friction velocity (which can be related to the flow
 179 velocity far above the canopy through a drag coefficient), α is the attenuation coefficient of velocity
 180 within the canopy (which increases with canopy density, MacDonald 2000) and z_0 is the canopy
 181 roughness length. Many attempts have been made to relate the displacement height and roughness
 182 length of vegetation canopies to the packing density of the obstacles as well as their arrangement &
 183 shape (e.g. Wooding et al. 1973). Similar studies are far less numerous for animal canopies, but
 184 similarly point out the difficulty in parameterizing drag and roughness in these systems (Rosman
 185 and Hench 2011). The mean velocity between the top of the canopy and the bottom of the
 186 logarithmic layer has not been fully described, but has been shown to contain characteristic features
 187 that engender strong similarities across the range of canopy flows (as discussed below).

188 The proposed exponential decay of horizontally-averaged velocity within the canopy (equation (3))
 189 is in fact a crude approximation to the highly-spatially-variable flow that develops in dense
 190 canopies. Figure 3 displays the horizontally-averaged flow between two-dimensional fixed rippled
 191 topography and shows that a steady return flow appears near the bed as the spacing between ripples
 192 decreases. This renders an exponential fit inappropriate deep within the roughness. Moreover,
 193 simulations show that the flow inside the canopy depends not only on the roughness density but also
 194 on ripple (i.e. obstacle) shape.

195

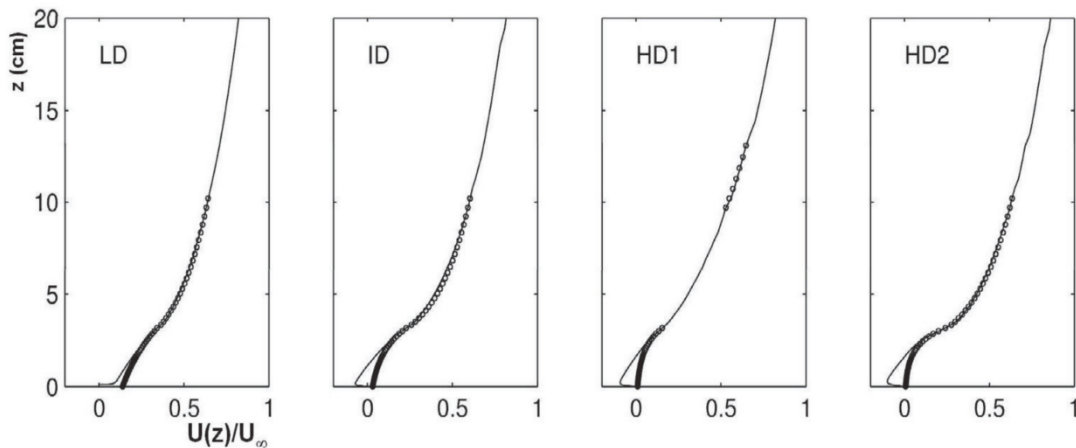
196

197

198

199

200 A)



207

208
209 B)
210
211
212
213
214
215
216
217
218
219
220
221
222
223
224
225
226
227
228
229
230
231
232
233
234
235
236
237
238
239
240

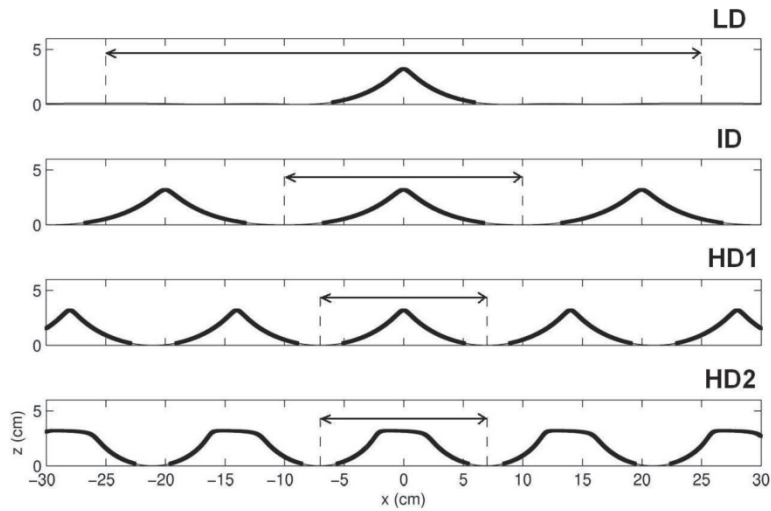


Figure 3: (A) Vertical profiles (solid lines) of the non-dimensional temporally- and horizontally-averaged longitudinal velocity ($U(z)/U_\infty$) for a steady flow of strength U_∞ above rippled beds with different densities. Fits for the logarithmic layer and for the exponential decay of velocity within the roughness are indicated by the circles; clearly, the exponential fit breaks down deep within the roughness (B) The varying densities and geometries of the rippled beds (LD = low density, ID = intermediate density, HD = high density, from Moulin et al., 2007, with kind permission of EDP Sciences).

Inherent similarities of canopy steady flows

A key feature of the mean velocity profile in canopy flows is the characteristic inflection point (i.e. a point of maximum velocity gradient) that is generated at the top of the canopy, the interface between the low speed in-canopy flow and high speed above-canopy flow. This inflection point yields the flow inherently unstable to Kelvin-Helmholtz-type vortices (Figure 4) that dominate the transport of mass and momentum across the top of the canopy (see, e.g., Ghisalberti and Nepf 2005, 2009).

241
242
243
244
245
246
247
248
249
250
251
252
253
254
255
256
257
258
259
260
261
262
263
264
265
266
267
268
269
270
271
272
273

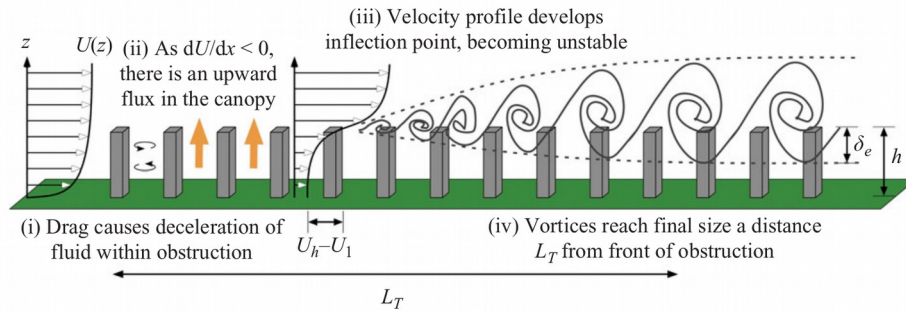


FIGURE 3. The evolution of flow along a submerged permeable medium. The distance required for full flow development L_T scales upon the drag length scale of the obstruction.

Figure 4: The streamwise evolution of steady canopy flow. The coherent vortices are a characteristic hydrodynamic feature of canopy flows (from Ghisalberti 2009, with kind permissions of Cambridge University Press).

Based on the dominance of these characteristic vortices, Ghisalberti (2009) demonstrated strong similarities across a range of canopy-type flows (termed ‘obstructed shear flows’), including atmospheric flows over forest canopies and aquatic flows over coral reefs and seagrass meadows. These similarities exist across a range of canopy scales (from $O(\text{mm})$ – $O(10 \text{ m})$) and provide predictive capability for the structure of the mean and turbulent flow in animal forests. For example, the thickness (δ_e) of the region within the canopy where the vortices drive rapid transport (Figure 4) is shown to scale inversely with canopy density (given here as the canopy frontal area per unit volume, a), according to:

$$\delta_e = 1/3 (C_D a)^{-1} \quad (4)$$

where C_D is the drag coefficient of the obstacles in the canopy. $(C_D a)^{-1}$ is termed the canopy drag length scale. Similarly, the intensity of vertical turbulent fluctuations (w_{rms}) at the top of the canopy is directly related to the friction velocity:

$$w_{rms} = 1.1 u_* \quad (5)$$

Canopy drag coefficients (as employed in (3)) are not typically known with a high degree of accuracy. Drag coefficients for certain (isolated) geometric shapes are well known, and simplifications have been made using morphological approximations. Vogel (1994) reports drag

274 coefficients of 0.74 for a rectangular solid, 0.76 for an erect cylinder and 0.32 for a hemisphere.
275 Such approximations may prove useful for some organisms in animal forests (e.g. hemisphere-like
276 stony corals, Hench and Rosman 2013) but, in general, canopies present the additional complexities
277 of (a) significant morphological complexity, including variation over height and (b) organisms
278 potentially existing in the wake of upstream elements, which can greatly affect the drag coefficient.
279 Drag estimation becomes complicated further when animal forests are comprised of organisms with
280 a range of ages, and hence a range of sizes and shapes, as is frequently observed in highly
281 diversified tropical environments. Thus, quantification of canopy drag coefficients has remained
282 elusive. Values of canopy drag coefficients ranging from 0.01 (Reidenbach et al. 2006) to 0.8
283 (MacDonald et al. 2006) have been estimated from flow measurements over coral reefs while
284 values used in reef flow modelling ranged from 0.02 to 0.1 (Rosman and Hench 2011).

285

286 *Variation of a steady flow with canopy density*

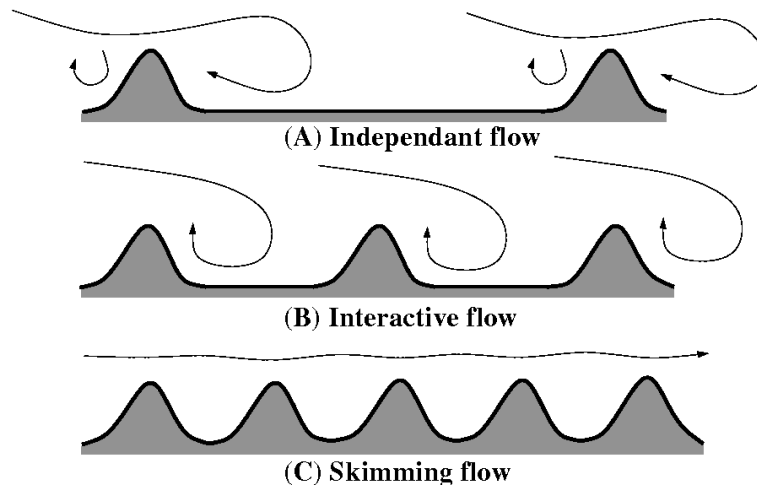
287

288 Qualitatively, three regimes of flow within and immediately above animal forests have been
289 identified. These regimes are distinguished by the packing density of the forest, and are schematized
290 in two dimensions in Figure 5 (adapted from Vogel 1994). At low density, each individual in the
291 forest is not in the wake of the closest upstream individual, and the forest impacts the mean velocity
292 profile only in the vicinity of the individual canopy elements. Both the displacement height and
293 roughness length remain small in this regime. As packing density increases, organism wakes begin
294 to interact, such that individual wakes can no longer be identified. The in-canopy flow becomes
295 strongly three-dimensional and local velocities depend strongly on the precise arrangement of
296 organisms. The apparent roughness increases in this regime, but the displacement height remains
297 small. As packing density increases further, forest drag produces a sufficiently strong blockage that
298 a ‘skimming’ flow (where the strength of the in-canopy flow is minimized) occurs above the
299 canopy. This corresponds to a decrease in the roughness length together with a rapid increase in the
300 displacement height. Density thresholds delineating these three flow regimes in real canopies
301 depend on the size of the wake that develops behind each organism, thus varying with organism size
302 and shape as well as flow speed. In the case of atmospheric flows over vegetation canopies, the
303 onset of skimming flows occurs for frontal area density (i.e. the canopy frontal area per unit bed
304 area) larger than 0.2 (MacDonald 2000).

305

306

307
308
309
310
311
312
313
314
315
316



317 Figure 5: Three typologies of flow modification in the vicinity of obstacles for increasing packing
318 density (adapted from Vogel 1994).

319

320 *Variation of a steady flow with canopy flexibility*

321

322 A significant complication in predicting the flow structure in animal forest canopies arises when
323 dealing with flexible organisms like soft-corals (Ghisalberti and Nepf 2006). It has been seen that,
324 even in steady flows, flexible canopies exhibit a coherent, large-amplitude waving (Ghisalberti and
325 Nepf 2002, Ghisalberti and Nepf 2004, termed the *monami* in vegetation canopies (Ackerman and
326 Okubo 1993). The generation mechanism of the *monami*, although still under debate (Singh et al.
327 2015), has been explained by the passage of the vortices at the top of the canopy, which create
328 strong sweeping motions as they pass (Ghisalberti and Nepf 2006). This coherent waving of flexible
329 canopies significantly modifies the structure of the mean and turbulent flow above and inside the
330 canopy, increasing (relative to rigid canopies) mean velocities inside the canopy and reducing the
331 friction velocity (Ghisalberti and Nepf 2009).

332

333 *Structure of the benthic boundary layer in oscillatory flows*

334

335

336 Marine animal forests are not exposed only to steady unidirectional flows (i.e. currents), but also to
337 oscillatory flows driven by wind-waves (shorter periods) and swell waves (longer periods). A
338 complete description of wave-driven flow requires two parameters: the amplitude of the orbital
339 velocity, U_w , and the wave period, T . As in steady flow, a boundary layer forms near the bed, within
340 which the wave orbital velocity decreases as the bed is approached.

341 In the absence of a canopy, boundary layers in oscillatory flow are considerably thinner than their
342 unidirectional counterparts. While tidal boundary layers frequently extend over several meters, the
343 boundary layer under a 10-second wave may extend over only a few centimeters. The thickness of a
344 turbulent oscillatory boundary layer can be approximated by $\sqrt{\frac{\tau_b}{\rho}} = \sqrt{\nu_t T}$ where ν_t is the eddy
345 viscosity (Nielsen 1992). With flow energy dissipated in such a thin layer, maximum bottom friction
346 velocities are generally an order of magnitude larger in wave flows than in the corresponding
347 unidirectional flow (Jonsson 1966). However, bottom friction velocities as all turbulent quantities
348 within a wave boundary layer exhibit oscillatory variations at half the wave periodicity (Sleath
349 1987). As a consequence of these time variations, and in contrast with steady boundary layers in
350 which turbulence intensity is fairly constant throughout fully developed boundary layers, time-
351 averaged turbulence intensity decay inversely with distance to the bed within a wave boundary layer
352 (Sleath 1987). However, when velocities are phase-averaged i.e. keeping track of the flow phase
353 along the periodic flow outside the boundary layer, the law of the wall (velocity log decay and
354 linear increase of mixing length) applies along a large part of the wave cycle (Jenssen et al. 1989).
355 These experiments partly validated various quasi-steady modelling of wave boundary layer (e.g.
356 Grant and Madsen 1979). However, describing with accuracy turbulent quantities within a turbulent
357 oscillatory boundary layer, and particularly the phase lagging of turbulent quantities across it,
358 motivated many more complex numerical modelling (reviewed by Fredsoe and Deigaard 1992,
359 Guizien et al., 2003).

360

361 In the presence of a canopy, a wave boundary layer is considerably less affected than a steady flow
362 boundary layer. The porous nature of the canopy, even at high densities, offers comparatively little
363 resistance to pressure transmission within the canopy, and velocity reduction inside the canopy will
364 be much smaller than in unidirectional flow (Lowe et al. 2005). No simple description exists for the
365 vertical profile of orbital velocity inside a canopy under wave-driven flow, although Lowe et al.
366 (2007) have developed a unique model for prediction of the overall velocity attenuation of canopies
367 in oscillatory flows. The model is based on wave energy dissipation from two sources, friction at
368 the top of the canopy and canopy element drag. Ultimately, however, its use relies on estimation of
369 friction and drag coefficients.

370 Similarly to steady flows, vortex generation at the top of the canopy is also observed under
371 oscillatory flows. This occurs when two key dimensionless parameters, namely the Reynolds
372 number and Keulegan-Carpenter number (the ratio of the timescale of flow oscillation to that of

373 shear layer formation), exceed threshold values such that an unstable shear layer forms on each
 374 wave half-cycle (Ghisalberti and Schlosser 2013). This means that vortices are preferentially seen in
 375 long and energetic waves over dense canopies.

376 In summary, developing predictive capability for the structure of the mean and turbulent flow in real
 377 marine canopies remains challenging. Nevertheless, a qualitative classification of the effect of the
 378 canopy on flow velocity and mixing can be proposed for animal forests (Table 1).

379

	Low population density	High population density
Wave-dominated flow	No significant attenuation of flow within canopy, enhanced mixing in canopy due to unsteady wakes.	Moderate flow attenuation within canopy, greatly enhanced mixing at top of canopy
Current-dominated flow	Flow speed reduced within canopy, fairly uniform rates of mixing through the canopy.	Flow speed strongly reduced within canopy, strong turbulent mixing in upper region of canopy, with reduced mixing near the bed.

380

381 Table 1: Summary of the key aspects of flow modification by animal forests.

382

383 3. The biogeochemistry inside and above the canopy of the animal forest

384

385 From a biogeochemical perspective, the analogy between terrestrial forests and marine animal
 386 forests is not straightforward given their opposite trophic pathways: trees as autotrophs synthesize
 387 organic matter from inorganic nutrients, absorbing CO₂, while animals degrade organic matter into
 388 inorganic compounds, releasing CO₂ (N.B. the analogy works somewhat better with tropical corals
 389 whose symbiotic association with autotrophic algae put them in the category of semi-autotrophs).
 390 Despite their reversed trophic pathways, an analogy between trees and marine animal forests can be
 391 based on their life-span; long-lived biota, either autotrophs or heterotrophs, act as carbon-sinks
 392 through carbon sequestration (albeit temporarily) as long as they grow, and thus influence the global
 393 carbon cycle in a similar manner. Furthermore, an increasing density of aquatic canopies is likely to
 394 shift their role in global biogeochemical cycles from carbon sink to carbon source. While the
 395 reduced flow and low turbulence deep in dense aquatic canopies can promote burial of undegraded
 396 particulate organic matter due to hypoxic conditions (carbon sink), higher levels of turbulence
 397 within canopies of intermediate density can maintain an oxygen supply sufficient to enhance the
 398 degradation of sedimenting organic matter (carbon source). The role of marine animal forests in

399 global biogeochemical cycles is also linked to their stability and to the diversity they host.
400 Biogeochemical conditions are essential drivers of the growth of large organisms and cell division
401 in micro-organisms. Therefore, it is critical that we understand how the regulation of mass transfer
402 inside and above canopies controls the uptake of biogeochemical compounds necessary for the
403 development of organisms living in or forming canopies, in order to predict their resilience to
404 disturbances (Holling 1973).

405

406 *Bulk mass transfer rates across canopy boundaries*

407

408 At the canopy scale, turbulent mixing regulates the exchange of dissolved and particulate species
409 across the top of the canopy boundaries. Indeed, mass transfer across the top of the canopy is
410 typically related by analogy to turbulent momentum transfer, which is governed by the interfacial
411 hydrodynamics. Turbulent momentum transfer (indicated by u_*) between the in-canopy and above-
412 canopy flows has been described through a momentum exchange velocity, U_E (Bentham and Britter
413 2003):

414

$$415 \quad u_*^2 = U_E (U_{ref} - U_c) \quad (6)$$

416

417 where U_{ref} is the flow velocity at $z = 2.5h$ (i.e. near the bottom of the logarithmic layer) and U_c is the
418 depth-averaged velocity inside the canopy.

419

420 By analogy, the rate of mass transfer (ϕ) of a dissolved compound across the top of the canopy is
421 thought to be controlled by the same exchange velocity as momentum and expressed by :

422

$$423 \quad \phi = U_E (C_c - C_{ref}) / Sc \quad (7)$$

424

425 (Moulin et al. 2007) where C_{ref} is the compound concentration at $z = 2.5h$ and C_c is the depth-
426 averaged concentration inside the canopy. The compound is characterized by its Schmidt number
427 (Sc), equal to the ratio of the kinematic viscosity of sea water (ν) to the diffusion coefficient of the
428 compound in sea water (D). This characterisation of mass transfer can also be described in terms of
429 the Stanton number (St), which represents the ratio of the mass transfer coefficient $\phi/(C_c - C_{ref})$ to
430 fluid advection (U_{ref}):

431

432 $St = \phi / [U_{ref} (C_c - C_{ref})] = U_E / (U_{ref} Sc),$ (8)

433

434 and depends only on the mean flow structure (and a Schmidt number correction). Given its practical
435 utility, formulations of the Stanton number as a function of canopy drag coefficient (as used by
436 Bilger and Atkinson 1992) have been developed to avoid the necessity of explicitly measuring the
437 in-canopy flow and mass transfer rate.

438 *Uptake inside the canopy*

439

440 For all the progress in understanding rates of mass transfer across canopy boundaries, downscaling
441 bulk fluxes at the canopy scale to the micro-scale heterogeneity of concentration within the canopy
442 remains a challenge. Within the canopy, transfer to organismal surfaces is expected to be regulated
443 by molecular diffusion in the organism's diffusive boundary layer, which extends over a portion
444 (approximately 10%) of the viscous sublayer. In canopies, the developed surface area where a
445 diffusive boundary layer (DBL) can be present is considerably enhanced compared to uncovered
446 beds and can reach 15 times the planar reef area (Dahl, 1973).

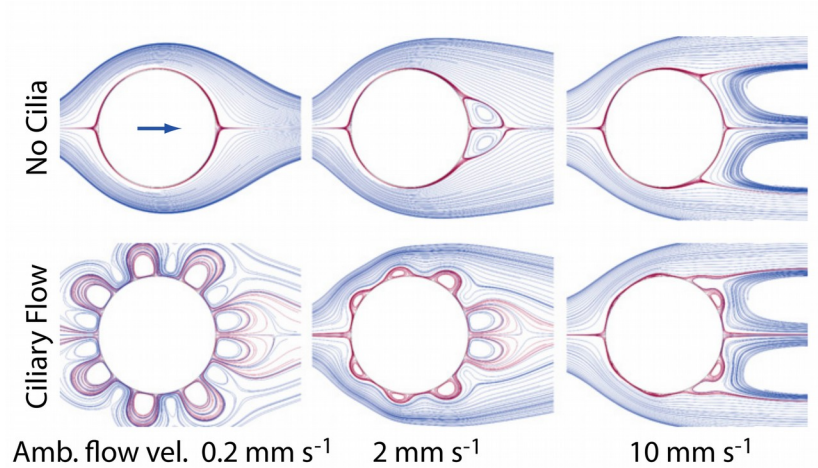
447 With the thickness of the DBL proportional to the viscous sublayer thickness, it decreases with the
448 local Reynolds number around the organism and will vary between canopy elements based on the
449 local flow speed and turbulence intensity. The lower the Reynolds number, the thicker the DBL.
450 Hence, the DBL is likely thicker on the upstream face of organisms spacing is large than in the
451 wake on the downstream face where turbulent detachment occurs and streamlines spacing is smaller
452 (Figure 6, upper panel). Active motile cilia on the epidermis of an organism disrupt the viscous and
453 diffusive boundary layers (Figure 6), increasing mass transport locally; up to a five-fold
454 enhancement of mass transfer rates to organism surfaces has been observed due to vortical ciliary
455 flows (Shapiro et al. 2014). Among cnidarians which often form animal forests, motile epidermal
456 cilia are present in scleratinian corals (Yonge 1930), but absent in octocorals (Lewis 1982). It is
457 worth noting that not all erected species rely on the physical disruption of the diffusive boundary
458 layer to increase mass transfer; many are active filter-feeders that create biomixing (Riisgard and
459 Larsen, this book).

460

461

462

463
464
465
466
467
468
469
470
471



472 Figure 6: Streamlines (shown in blue) from numerical simulations of flow around a coral branch
473 (diameter = 5 mm). Streamline spacing can be taken as proxy for DBL thickness: the greater the
474 spacing, the thicker the DBL. Ciliary vortical flows (lower panel) significantly impact the flow
475 topology and decrease the DBL thickness at low-to-moderate ambient flow velocities, relative to the
476 no-cilia case (upper panel). The arrow marks the direction of the ambient flow. Streamlines shown
477 in red are those passing within 50 μm of the branch (from Shapiro et al. 2014, with kind permission
478 of PNAS Editions)..

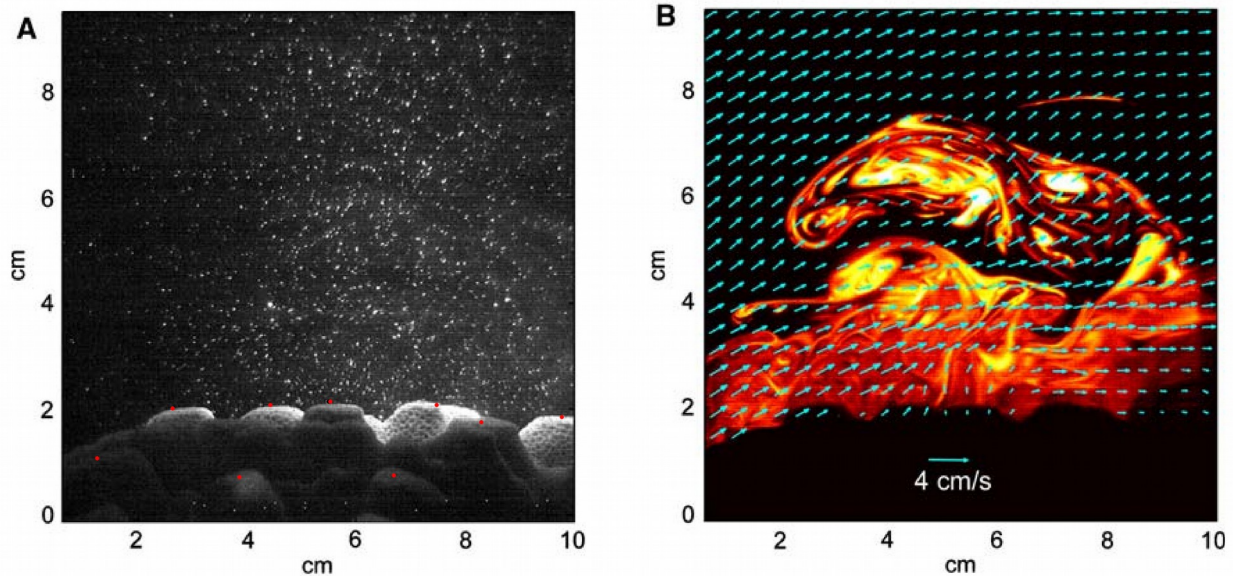
479
480

481 In addition to the spatial heterogeneity of mass transfer inside the canopy, the canopy organisms
482 contribute to strong concentration gradients through their consumption or production. Coral polyps
483 (indicated by red dots in Figure 7A), where biogeochemical transformations take place through
484 respiration, calcification, uptake and release of organic and inorganic forms of phosphorous and
485 nitrogen, form a complex three-dimensional distribution of concentration (Figure 7B).

486

487 Mapping the micro-scale physical and chemical environment that organisms experience requires
488 high-resolution, 3D measurements of both flow and concentration. The current capacity is limited to
489 simultaneous 2D visualization of flow and concentration through a combination of Particle Image
490 Velocimetry (PIV) and Particle Laser Induced Fluorescence (PLIF, e.g. Koehl and Reidenbach
491 2007, Figure 7B). Significant advances should be sought to improve the 3D mapping of flow and
492 concentration, which may come from medical (Positron Emission Tomography) or material science
493 (Raman spectrometry, Du et al. 2015) technologies.

494



496 Figure 7: Example of simultaneous PIV and PLIF measurements over *Porites compressa* coral in a
 497 wave-dominated flow (with a weak current present) in a flume. (A) A PIV frame, on which opening
 498 polyps are indicated by red dots. (B) A PLIF image of dye concentration released from the coral
 499 coating, recorded 0.02 s after the image shown in A. The velocity vectors during this interval are
 500 shown in blue (from Koehl and Reidenbach, 2007, with kind permissions of Springer).

501

502 *Relating bulk mass transfer across the canopy to local mass transfer limitations*

503 An important application of the Stanton number characterisation of bulk mass transfer across
 504 canopies was in the demonstration that local nutrient uptake by coral reef organisms is frequently
 505 mass-transfer-limited, and not biologically-controlled. It has been shown that Stanton numbers for
 506 phosphate in experimental coral reefs (assuming infinitely rapid uptake, i.e., taking $C_c = 0$) agree
 507 well with those estimated from engineering formulations that only consider the hydrodynamic
 508 influence of the reef roughness (Bilger and Atkinson 1992). Other methods for quantifying the
 509 influence of fluid-canopy interactions on nutrient supply can be based on comparisons of timescales
 510 of nutrient consumption (if known) and canopy flushing (e.g. Kregting et al. 2011). Mass transfer
 511 limitation on reef flats has been shown for ammonia and nitrate, including under waves (Falter et al.
 512 2004), demonstrating the high demand for these compounds in coral reefs. Similarly, mass transfer
 513 limitation has been shown for ammonia in seagrass and macroalgae canopies (Cornelisen and
 514 Thomas 2009; Stephens and Hepburn 2014). For heterotrophic forest-forming species, such as
 515 Mediterranean gorgonians, the validity of assuming mass transfer limitation for basic resources

516 (oxygen and organic compounds) must be investigated.

517 Canopy uptake will not always be physically-limited, however; in such cases, direct measurements
518 of mass transfer into the canopy are required. Eddy correlation techniques allow direct measurement
519 of turbulent diffusive fluxes of a compound, provided a high-frequency, small-scale technique exists
520 to measure the compound concentration and its turbulent fluctuations. In marine systems, such
521 measurements can only be provided by micro-electrode sensors, which effectively limits the
522 technique to quantification of fluxes of dissolved oxygen (Berg et al. 2003). Importantly, eddy
523 correlation techniques allow quantification of local fluxes under both wave- and current-dominated
524 flows, unlike the exchange velocity model in (6), which only applies to steady flows. The eddy
525 correlation approach was used to monitor spatial and temporal variability of respiration and
526 photosynthesis rates over the slope and crests of a coral reef (Long et al. 2013). In this study,
527 respiration rates increased with current velocity, suggestive of mass transfer limitation. Rates of
528 respiration and gross primary production were higher on the reef crest (dominated by gorgonians
529 and soft-corals) than on the reef slope (dominated by sand and pavement).

530

531 4. Living in the canopy of the animal forest

532

533 Habitat complexity has long been recognized as increasing biodiversity and biomass, explained
534 through the provision of a diversity of niches (MacArthur and MacArthur 1961). Aquatic canopies
535 built by flora or fauna display structural complexity and have been shown to host higher diversity
536 and biomass than bare beds (Benedetti-Cecchi et al. 2001; Emslie et al. 2014). Yet, the relationship
537 between canopy complexity (measured through precise canopy descriptors) and the hosted diversity
538 and biomass still needs to be defined. In a recent study, the overall fish population biomass (driven
539 by large fishes) was positively correlated with the density of kelp stipes forming a canopy over
540 temperate rocky reefs (Trebilco et al. 2015). The fish population structure, however, was more
541 closely correlated to the roughness of the under-canopy rocky substratum. While this study is
542 clearly a step towards more quantitative description of understorey species habitat, it highlights the
543 lack of a mechanistic conceptualization of habitat complexity, one that integrates the effects of the
544 underlying substratum roughness and the canopy to predict the overall flow structure. Moreover,
545 although canopy density likely influences the living conditions of fishes inside the canopy, the
546 increase of fish biomass with canopy density is not straightforward given the nonlinear effect of
547 density on the canopy flow structure. Indeed, turbulence intensity first increases with density (as
548 indicated by an increase in roughness length) but then suddenly decreases with the onset of

549 skimming flow in dense canopies (a decrease in roughness length, Vogel 1994).

550 Elucidating the functional role of canopies requires consideration of the combination of all physical
551 and chemical factors that are (1) locally- or globally-modified within a canopy and (2) that define
552 the fundamental niche of a hosted species. A fundamental niche (*sensu* Hutchinson 1957) is defined
553 as the set of abiotic conditions in which a species can live. Fundamental niche explorations should
554 rely on different experimental or observational strategies according to the motility of hosted species.
555 For sessile species, fundamental niches should be sought with an Eulerian approach; that is,
556 monitoring in fixed locations, determining regions where temporal variations in physical and
557 chemical conditions are within acceptable ranges. For mobile species, fundamental niches should be
558 sought with a Lagrangian approach; that is, monitoring conditions along potential organism paths.

559

560 *Living in a sparse animal forest*

561 In marine animal forests with low population density, the flow intensity will display localized
562 variations, creating a dependence on organism arrangement of rates of mass transfer to organism
563 surfaces. Hosted and more precisely-associated fauna and flora are expected to display a spatial
564 structure reflecting the wakes developing behind each individual. In such open forests, mass
565 transfer into the canopy will not be significantly affected and the biogeochemical conditions are
566 expected to be similar to those in the absence of the animal forest(except in individuals wake), such
567 that the physical conditions will be dominant in structuring the biota, particularly in determining
568 colonization processes (settlement and post-settlement survival). Individual wakes should increase
569 local larval retention and could potentially facilitate densification of the forest by self-recruitment
570 of the canopy-forming species as long as intra-specific competition remains small. However, such
571 densification may be slow compared to algal growth in photic areas, suggesting that shallow animal
572 forests would be less resilient to perturbation than deeper ones.

573

574 *Living in a moderately populated animal forest*

575 In marine animal forests of intermediate population density, in which there is significant wake
576 interaction, the patchiness of mass transfer into the canopy and flow intensity (together with some
577 light penetration) should promote diversification of trophic niches, enabling the development of
578 slow growing sessile autotrophs competing for space with sessile heterotrophs. In this context,
579 despite high local retention of larvae by the animal forest, recruitment success will probably be low
580 due to strong intra- and inter-specific competition. The settlement of sessile heterotroph larvae in
581 these environments should be favored in regions of rapid mass transfer into the canopy. The larvae

582 of some species are able to respond sufficiently quickly to turbulent fluctuations so as to change and
583 adapt their locomotory behaviour to more precisely follow chemical cues to appropriate sites
584 (Koehl et al. 2007). The ability of larvae with low motility to maintain themselves in the appropriate
585 Lagrangian niche seems to depend on the larval sinking speed: only those larvae with a sufficiently
586 high density or rapid behavioural changes (e.g. velum retraction, cessation of swimming) will settle
587 rapidly enough. Patchy flow conditions and visual occlusion in less dense canopies should limit the
588 size of highly mobile species (like fishes) seeking low-flow refuge in animal forests. In summary,
589 marine animal forests of intermediate population density are expected to be characterized by (1) a
590 high diversity of sessile species, autotrophic and heterotrophic, whose distribution could reflect the
591 colonization ability of larvae advected from distant sites, and (2) strong intra- and inter-specific
592 competition. Hosted mobile species are expected to be diversified, due to the variety of trophic
593 resources associated with the diversity of sessile species and the spatial variability of the flow
594 (Finelli et al. 2009). Such hosted species are expected to be limited in number and size, depending
595 on the size and shape of the canopy-forming organisms. In marine animal forests of intermediate
596 density, the choice of spatial and temporal scales used to describe in-canopy conditions is incredibly
597 important, as canopy-averaged values may differ greatly from those actually experienced by
598 organisms. Upscaling procedure should take into account not only average but also variance and co-
599 variance descriptors. Quantile descriptors should also be considered as to express the proportion of
600 time or space over which given conditions are experienced.

601

602 *Living in a dense animal forest*

603 In dense canopies (of either autotrophs or heterotrophs), the reduction of rates of mass transfer near
604 the bed associated with the low in-canopy flow is expected to lead to the accumulation of
605 compounds excreted by the canopy-forming species. Similarly, the consumption of compounds
606 useful to the canopy-forming species can lead to their depletion. Local modification of the
607 biogeochemical and mass transfer conditions below dense assemblages of macroalgae growing on
608 sessile corals was found to be deleterious to the development of sessile corals, due to the reduction
609 in oxygen concentration and increase in dissolved organic carbon concentration (Hauri et al. 2010).
610 Combining limited diffusion and high rates of consumption, sessile species hosted in dense
611 canopies are expected to be limited to those having a different trophic regime than the canopy-
612 forming species. However, near the bed in dense heterotrophic marine forests, low light conditions
613 should also prevent the development of algae. In the absence of competition with algae in a low
614 flow environment, bacteria associated with hypoxic environments will likely be favored, in turn
615 leading to low biomass and a uniform composition of sessile species. One could expect a dense

616 canopy to be monospecific, or at least formed by species sharing similar growth traits. Indeed, a
617 canopy will adjust so as to have a large surface area in the the high-velocity, turbulent region of the
618 canopy flow, where the DBL around the organism surface is thin. Such a mechanism was proposed
619 recently to explain the existence of the oldest known marine animal forest in the deep ocean of the
620 Precambrian era (Ghisalberti et al. 2014). In the low-flow and nutrient-rich conditions of the
621 Precambrian ocean, tall rangeomorphs could have grown up to 2 m relying on osmotic uptake only,
622 due to an increased mass transfer to the organism surface resulting from a thinned DBL. As a
623 consequence of limited diffusion and flow velocity in the lower part of the canopy, one can expect
624 dense canopies to be cleared of smaller sessile species, freeing space for mobile species like fishes
625 looking for shelter from predators and low flow conditions to rest. The amount of open space in the
626 lower canopy might even increase as the canopy grows, as some canopy-forming species with a
627 tree-like shape experience population density decay through a self-thinning mechanism (Cau et al.
628 2016). In this case, the hosted biomass is expected to increase with the growth of the canopy-
629 forming species. In summary, one could expect dense marine animal or vegetal forests to (1) be
630 composed of sessile species of similar height, (2) host a diverse and large biomass of highly mobile
631 species like fishes that are using the canopy as a refugia, and (3) a diverse microbiota subsisting on
632 by-products of macrobiota function. .

633

634

635 5. Conclusions and Future directions

636

637 Local modification of the physical and biogeochemical environment by erect animals living on the
638 sea floor has long been recognized as a key factor generating high biodiversity and biomass in the
639 understory. While there is a fairly comprehensive understanding in the environmental fluid
640 mechanics community of the modification of the flow structure generated by these animal forests,
641 these modifications are not well-known amongst the biological community studying these diverse
642 assemblages. In this sense, marine animal forests are archetypal of ecosystems whose study requires
643 more interdisciplinarity and reciprocal pedagogy to advance knowledge. Indeed, going beyond the
644 term 'habitat complexity' to explain species associations in a unified framework to yield a typology
645 of forest requires an understanding of physically-relevant parameters such as canopy planar and
646 frontal density, roughness and drag coefficients, and non-dimensional parameters such as the
647 Reynolds, Keulegan-Carpenter and Stanton numbers.

648 Research into the physical and biogeochemical environments around scleratinians has demonstrated

649 the relevance of such an interdisciplinary approach in explaining species function. Drawing
650 scientific attention to scleratinians in the last 40 years was possible given the climatic and
651 overfishing threats that they face. However, other marine animals, such as gorgonians, soft-corals
652 and sponges (Maldonado et al., in this book), form animal forests that may colonize places freed up
653 by scleratinians and provide an alternative complex habitat for understory species. The flexibility
654 of soft-coral species contrasts with the stiffness of scleratinian species, making their hydrodynamic
655 influence similar to that of vegetation canopies.

656 The ultimate goal of such interdisciplinary research should be to develop models of marine animal
657 forest functioning, and to compare predictions and observations of niche extent in a meta-
658 community approach. Such models will then be useful in the prediction of biodiversity evolution
659 under climatic and anthropogenic stresses, thereby assisting conservation efforts.

660

661

662 References

663

664 Ackerman JD, Okubo A. Reduced mixing in a marine macrophyte canopy. *Funct. Ecol.* 1993 ;7,
665 305–309.

666

667 Bartholomew A. New dimensionless indices of structural habitat complexity: predicted and actual
668 effects on a predators foraging success. *Mar. Ecol. Progr. Ser.* 2000 ; 206: 45-58.

669

670 Benedetti-Cecchi L, Pannacciulli F, Bulleri F, Moschella PS, Airoldi L, Relini G, Cinelli F.
671 Predicting the consequences of anthropogenic disturbance: large-scale effects of loss of canopy
672 algae on rocky shores. *Mar. Ecol. Prog. Ser.* 2001 ; 214, 137 – 150.

673

674 Bentham T, Britter R. Spatially averaged flow within obstacle arrays. *Atmos. Environ.* 2003 ;37 :
675 2037-2043.

676

677 Berg P, Roy H, Janssen F, Meyer V, Jorgensen BB, Huettel M, De Beer D. Oxygen uptake by
678 aquatic sediments measured by a novel non-invasive eddy correlation technique. *Mar Ecol Prog*
679 *Series* 2003;261:75-83

680

681 Beukers JS, Jones GP. Habitat complexity modifies the impact of piscivores on a coral reef fish
682 population. *Oecologia*, 1997 ; 114, (1): 50-59

683

684 Bilger RW, Atkinson MJ. Anomalous mass transfer of phosphate on coral reef flats. *Limnol*
685 *Oceanogr.* 1992 ; 37(2) : 261-272

686

687 Bruno JF. Whole-community facilitation through substrate stabilization by the intertidal grass
688 *Spartina alterniflora*. *Ecology* 2000 ; 81: 1179-1192.

689

690 Bruno JF, Bertness MD. Habitat modification and facilitation in benthic marine communities. In:
691 Bertness M.D., M.E. Hay, and S.D. Gaines (eds.) *Marine Community Ecology*. 2001 ; Sinauer,
692 Sunderland, MA: 201-218.

693

694 Cau A, Bramanti L, Angiolillo M, Bo M, Canese S, Cuccu D, Cannas R, Follesa MC, Guizien K.
695 Habitat constraints and self-thinning shape Mediterranean red coral deep population structure:
696 implications for conservation practice. *Scientific Reports*. 2016; 6 : 23322-1-10

697

698 Cerrano C, Danovaro R, Gambi C, Pusceddu A, Riva A, Schiaparelli S. Gold coral (*Savalia*
699 *savaglia*) and gorgonian forests enhance benthic biodiversity and ecosystem functioning in the
700 mesophotic zone. *Biodiversity and Conservation* 2010; 19(1): 153-167.

701

702 Cheng H, Castro IP. Near wall flow over urban-like roughness. *Boundary-layer Meteorology* 2002;
703 104, 2: 229–259.

704

705 Cordes EE, McGinley MP, Podowski EL, Becker EL, Lessard-Pilon S, Viada ST, Fisher CR. Coral
706 communities of the deep Gulf of Mexico. *Deep Sea Research Part I: Oceanographic Research Pa-*
707 *pers.* 2008 ; 55 (6): 777-787.

708

709 Cornelisen CD, Thomas FIM. Prediction and validation of flow-dependent uptake of ammonium
710 over a seagrass-hardbottom community in Florida Bay. *Mar Ecol Prog Series* 2009 ; 386:71-81

711

712 Dahl LA. Surface area in ecological analysis : quantification of benthic coral-reef algae. *Mar Biol.*
713 1973 ; 23: 239-249

714

715 Dennison WC, Barnes DJ. Effect of water motion on coral photosynthesis and calcification. *J. Exp.*

716 Mar. Biol. Ecol. 1988 ; 115: 67-77.
717
718 Du Z, Li Y, Chen J, Guo JJ, Zheng RE. Feasibility investigation on deep ocean compact
719 autonomous Raman spectrometer developed for in-situ detection of acid radical ions. Chinese
720 journal of Oceanology and Limnology. 2015 ; 33(2):545-550
721
722 Duarte CM. Marine biodiversity and ecosystem services: an exclusive link. [Journal of Experimental](#)
723 [Marine Biology and Ecology](#) 2000 ; [250 \(1-2\)](#): 117-131.
724
725 Eckman JE. Flow disruption by an animal- tube mimic affects sediment bacterial colonization. J.
726 Mar. Res. 1985 ; 43: 419-435.
727
728 Eckman JE, Duggins OD, Sewel AT Ecology of understory kelp environments. Effects of kelps on
729 flow and particle transport near the bottom. J. Exp. Mar. Biol. Ecol. 1989 ; 129: 173-187
730
731 Emslie MJ, Alistair JC, Johns KA. Retention of habitat complexity minimizes disassembly of reef
732 fish communities following disturbances : a large-scale natural experiment. Plos One. 2014 ; 9(8) :
733 e105384-1-9
734
735 Fabricius KE, Metzner J. Scleractinian walls of mouths: Predation on coral larvae by corals. Coral
736 Reefs. 2004 ; 23:245-248
737
738 Falter JL, Atkinson MJ, Merrifield MA. Mass-transfer limitation of nutrient uptake by a wave-
739 dominated reef flat community. Limnol. Oceanogr. 2004 ; 49(5) : 1820-1831
740
741 Finelli CM, Clarke RD, Robinson HE, Buskey EJ. Water flow controls distribution and feeding
742 behavior of two co-occurring coral reef fishes : I. Field Measurements. Coral reefs. 2009 ; 28 : 461-
743 473
744
745 Fredsoe J, Deigaard R. Mechanics of coastal sediment transport. Advanced Series on Ocean
746 Engineering. 3. 1992. World Scientific Publishing Co. Pte. Ltd.
747
748 Freiwald A, Roberts JM. (Eds). Cold water corals and ecosystems. 2005. Springer publishing.
749

750 Ghisalberti M Obstructed shear flows: similarities across systems and scales. *J. Fluid Mech.* 2009 ;
751 641:51-61.
752
753 Ghisalberti M, Nepf H. The structure of the shear layer in flows over a rigid and flexible canopies.
754 *J. Geophys. Res. Oceans.* 2002 ; 107(C2): 3011-1-11.
755
756 Ghisalberti M, Nepf H. The limited growth of vegetated shear layers. *Water Resources Res.* 2004 ;
757 40(7): W07502-1-12.
758
759 Ghisalberti M, Nepf H. The structure of the shear layer in flows over a rigid and flexible canopies.
760 *Env. Fluid Mech.* 2006 ; 6: 277-301.
761
762 Ghisalberti M, Schlosser T. Vortex generation in oscillatory canopy flow. *J. Geophys. Res. Oceans.*
763 2013 ;118:1534-1542, doi : 10.1002/jgrc.20073.
764
765 Ghisalberti M, Gold DA, Laflamme M, Clapham ME, Narbonne GM, Summons RE, Johnston DT,
766 Jacobs DK. Canopy flow analysis reveals the advantage of size in the oldest communities of multi-
767 cellular Eukaryotes. *Current biology.* 2014 ;24:305-309.
768
769 Grant WD, Madsen OS. Combined wave and current interaction with a rough bottom. *J Geophys*
770 *Res.* 1979 ; 84(C4):1797-1808
771
772 Gutt J, Cummings V, Dayton, Isla E, Jentsch A, Sciaparelli S. Antarctic marine animal forests : three-
773 dimensionnal communities in Southern ocean ecosystems. *Marine animal forests.* S. Rossi (ed.)
774 Springer International Publishing Switzerland 2015. DOI 10.1007/978-3-319-170001-5_8-1
775
776 Guizien K, Dohmen-Janssen M, Vittori G. 1DV bottom boundary layer modeling under combined
777 wave and current : turbulent separation and phase lag effects. *J. Geophys. Res.* 2003 ;108 (C1), 16 :
778 1-15
779
780 Goreau TJ. Control of atmospheric carbon-dioxide. *Global environmental change – human and*
781 *policy dimensions.* 1992 ; 2(1) : 5-11.
782
783 Hauri C, Fabricius KE, Schaffelke B, Humphrey C. Chemical and physical environmental

784 conditions underneath mat- and canopy-forming macroalgae, and their effects on understory
785 corals. Plos One 2010 ; 5 (9) : e12685, 1-9
786
787 Hench JL, Rosman JH. Observations of spatial flow patterns at the coral colony scale on a shallow
788 reef flat. J. Geophys. Res. 2013 ; 118, 1142-1156, doi:10.1002/jgrc.20105
789
790 Holling CS. Cross-scale morphology, geometry and dynamics of ecosystems. Ecol. Monogr. 1992 ;
791 62: 447-502.
792
793 Holling CS Resilience and stability of ecological systems. Annual Review of Ecology and
794 Systematics. 1973 ; 4: 1-23.
795
796 Hutchinson GE. Concluding remarks. Cold Spring Harbor Symposia on Quantitative Biology.
797 1957; 22(2) :415–427
798
799 Jenssen BL, Sumer BM, Fredsoe J. Turbulent oscillatory boundary layers at high Reynolds
800 numbers. J Fluid Mech. 1989 ; 206:265-297.
801
802 Jones CG, Lawton JH, Shachak M. Organisms as ecosystem engineers. Oikos. 1994 ; 69 (3):373-
803 386.
804
805 Jones CG, Lawton JH, Shachak M. Positive and negative effects of organisms as physical
806 ecosystem engineers. Ecology. 1997 ; 78 (7):1946-1957.
807
808 Jonsson IG. Wave boundary layers and friction factors. Proc 10th Conf Coastal Eng. 1966 : 127-
809 148.
810
811 Kerry JT, Bellwood DR. The effect of coral morphology on shelter selection by coral
812 reef fishes. Coral reefs. 2012 ; 31:415-424
813
814 Koehl MAR, Reidenbach MA. Swimming by microscopic organisms in ambient water flow. Exp.
815 Fluids. 2007 ; 43:755-768
816
817 Koehl MAR, Strother JA, Reidenbach MA, Koseff JR, Hadfield MG. Individual-based model of

818 larval transport to coral reefs in turbulent, wave-driven flow: behavioral responses to dissolved
819 settlement inducer. *Mar Prog Ecol Series*. 2007 ; 335:1-18
820

821 Kolmogorov AN. Local structure of turbulence in incompressible viscous fluid for very large
822 Reynolds number. *Doklady Akademia Nauk SSSR*. 1941 ; 30:299-303.
823

824 Kregting LT, Stevens CL, Cornelisen CD, Pilditch CA, Hurd CL. Effects of a small-bladed
825 macroalgal canopy on benthic boundary layer dynamics : implications for nutrient transport. *Aquat*
826 *Biol* 2011;14(1):41-56.
827

828 Lawton JH. What do species do in ecosystems ? *Oikos*. 1994 ; 71(3) : 367-374
829 Long MH, Berg P, de Beer D, Zieman JC. In situ coral reef oxygen metabolism : an eddy
830 correlation study. *Plos One*. 2013 ; 8(3) : e58581, 1-11
831

832 Lewis JB. Feeding behaviour and feeding ecology of the octocorallia (coelenterata: Anthozoa). *J*
833 *Zool*. 1982 ; 196(3):371–384.
834

835 Lowe RJ, Koseff JR, Monismith SG. Oscillatory flow through submerged canopies. Part 1. Velocity
836 structure. *J. Geophys. Res*. 2005;110:C10016, doi:10.1029/2004JC002788
837

838 Luckenbach MW. Sediment stability around animal tubes: The roles of hydrodynamic processes and
839 biotic activity. *Limnol. Oceanogr*. 1986 ; 31: 779-787.
840

841 MacArthur R, MacArthur JW. On bird species-diversity. *Ecology* 1961 ; 42(3) : 594-&
842

843 Mac Donald RW. Modelling the mean velocity profile in the urban canopy layer. *Boundary Layer*
844 *Meteorology* 2000 ; 97:25-45.
845

846 Mac Donald CB, Koseff, JR, Monismith SG. Effects of the depth to coral height ratio on drag
847 coefficients for unidirectional flow over coral. *Limnol. Oceanogr*. 2006 ; 51:1294-1301.
848

849 Maldonado M, Aguilar R, Bannister RJ, Bell JJ, Conway KW, Dayton PK, Diaz C, Gutt J, Kelly M,
850 Kenchington ELR, Leys SP, Pomponi SA, Rapp HS, Rützler K, Tendal OS, Vacelet J, Young CM.
851 Sponge grounds as key marine habitats : a synthetic review of types, structure, functional roles, and

852 conservation concerns. Marine animal forests. S. Rossi (ed.) Springer International Publishing
853 Switzerland 2015. DOI 10.1007/978-3-319-170001-5_24-1
854

855 Monismith SG Hydrodynamics of coral reefs. Annu. Rev. Fluid Mech. 2007 ; 39:37–55
856

857 Moulin FY, Guizien K, Thouzeau G, Chapalain G, Mülleners K, Bourg C. Impact of an invasive
858 species *Crepidula fornicata* on the hydrodynamics and transport properties of the benthic layer.
859 Aquatic Liv. Res. 2007; 20(1): 15-31
860

861 Myhrvold CL, Stone HA, Bou-Zeid E. What is the use of elephant hair ? Plos One. 2012 ; 7(10) :
862 e47018-1-6.
863

864 Nepf H, Ghisalberti M, White B, Murphy E. Retention time and dispersion associated with
865 submerged aquatic canopies. Water Resour. Res. 2007 ; 43, W04422.
866

867 Nielsen P. Coastal bottom boundary layers and sediment transport. Advanced Series on Ocean
868 Engineering. 4. 1992. World Scientific Publishing Co. Pte. Ltd.
869

870 Nikuradse J. “Stromungsgesetze in glatten und rauhen rohren.”VDI-Forschungsh., 361, Berlin (in
871 German). 1933.
872

873 Raupach MR, Thom AS, Edwards I. A wind-tunnel study of turbulent flow close to regularly
874 arrayed rough surfaces. Boundary-Layer Meteorology. 1980 ; 18 : 373-397.
875

876 Reidenbach MA, Monismith SG, Koseff JR, Yahel G, Genin A. Boundary layer turbulence and flow
877 structure over a fringing coral reef, Limnol. Oceanogr. 2006 ; 51(5), 1956–1968,
878 doi:10.4319/lo.2006.51.5.1956
879

880 Riisgard HU, Larsen PS. Filter-feeding zoobenthos and hydrodynamics. Marine animal forests. S.
881 Rossi (ed.) Springer International Publishing Switzerland 2015. DOI 10.1007/978-3-319-170001-
882 5_19-1
883

884 Rosman JH, Hench JL. A framework for understanding drag parameterizations for coral reefs. J.
885 Geophys. Res. 2011 ; 116, C08025, doi:10.1029/2010JC006892

886
887 Ross S, Quattrini A. The fish fauna associated with deep coral banks off the southeastern United
888 States. *Deep Sea Research I*. 2007 ; (54): 975-1007.
889
890 Scinto A, Bertolino M, Calcinai B, Huete-Stauffer C, Previati M, Romagnoli T, Cerrano C. Role of
891 paramuricea clavata forest in modifying the coralligenous assemblages. Proceedings of the first
892 Mediterranean symposium on the conservation of the coralligenous and other calcareous bio-
893 concretions. 2009 ; Tabarka January 15-16 2009.
894
895 Shapiro OH, Fernandez VI, Garren M, Guasto JS, Debaillon-Vesque FP, Kramarsky-Winter E, Vardi
896 A, Stocker R. Vortical ciliary flows actively enhance mass transport in reef corals. *Proc Nat Acad*
897 *Science of the United States of America* 1930 ; 111(37) : 13391-13396
898
899 Shashar N, Kinane S, Patterson PLJ, Patterson MR. Hydromechanical boundary layers over a coral
900 reef. *J. Exp. Mar. Biol. Ecol.* 1196 ;199: 17-28.
901
902 Singh R, Bandi MM, Mahadevan A, Mandre S. Linear stability analysis for monami in submerged
903 seagrass bed. *J. Fluid Mech.* 2016 ;786:R1, doi:10.1017/jfm.2015.642
904
905 Sleath J.F.A. *Sea bed mechanics (Ocean Engineering)*. Eds Wiley-Interscience. 1984 ; 335 p.
906
907 Sleath J.F.A. Turbulent oscillatory flows over rough beds. *J Fluid Mech.* 1987 ; 182:369-409
908
909 Smith F, Witman JD. Species diversity in subtidal landscapes: Maintenance by physical processes
910 and larval recruitment. *Ecology* 1999 ; 80: 51-69.
911
912 Stephens TA, Hepburn CD. Mass-transfer gradients across kelp beds influence *Macrocystis pyrifera*
913 growth over small spatial scales. *Mar Ecol Prog Series* 2014 ; 515:97-109.
914
915 Thistle D, Eckman JE. The effect of a biologically produced structure on the benthic copepods of a
916 deep-sea site. *Deep Sea Res.* 1990 ; 37: 541-554.
917
918 Trebilco R, Dulvy NK, Steward H, Salomon AK. The rôle of habitat complexity in the size structure
919 of a temperate reef fish community. *Mar Ecol Prog Series* 2015 ; 532:197-211
920

- 921 Vogel S. *Life in Moving Fluids* (2nd edn). Princeton: Princeton University Press ; 1994
922
- 923 Wilcox DC. *Turbulence modelling for CFD* (2nd edn). DCW Industries ; 2000
924
- 925 Wooding RA, Bradley EF, Marshall JK. Drag due to regular arrays of roughness elements of
926 varying geometry, *Boundary-Layer Meteorol.* 1973 ; 5 : 285–308.
927
- 928 Yonge CM. *Studies on the physiology of corals. I. Feeding mechanisms and food.* Great Barrier
929 Reef Expedition 1928-29, *Scientific Report 1930* ;[British Museum (Natural History), London,
930 UK], pp 13–57.
931